

## **Application and verification of ECMWF products 2014**

Israel Meteorological Service (IMS),

### **1. Summary of major highlights**

- Compared to 2013 there is an improvement in temperature, humidity and wind speed predictability for a lead time of 10 days. RMSE's are reduction for temperature by about 0.5°C, for humidity by about 2% and for wind speed by about 0.3 m/s.
- ECMWF deterministic runs are used to issue most of the operational forecasts at IMS. Fire danger indices are issued based on IFS forecasts after 7 day running average bias correction.
- Nowcasting is performed by the INCA (Integrated Nowcasting through Comprehensive Analysis) system, which is based on IFS forecasts and automatic station data from Israel.
- UV index is calculated on the bases of ECMWF global radiation via empirical functions.
- Very high correlation ( $r = 0.95-0.96$ ) was found between ECMWF WAM Significant Wave Height (SWH) forecasts and near shore buoy observations.
- Unlike last year the seasonal forecast was skilful for winter and summer temperatures and winter precipitation.

### **2. Use and application of products**

#### **2.1 Post-processing of model output**

##### *2.1.1 Statistical adaptation*

IFS forecasts for 2m temperature, 2m humidity, 10m wind are corrected with the last 7 days running bias. The results together with cloudiness, precipitation amount and duration, are ingested to the US National Fire Danger Rating System (NFDRS). This system is used to provide a measure of the relative seriousness of burning conditions and the threat of fire. We calculated the IC (Ignition Component) and BI (Burning Index) for the previous 4 years to create indexes climatology. The vales above the 90<sup>th</sup>percentile were defined as “high” as the above the 98<sup>th</sup>percentilewere defined as “extreme”. Comparing daily IC and BI forecasts to their “climatic” values provides forecasted maps of fire probability (fig. 1).

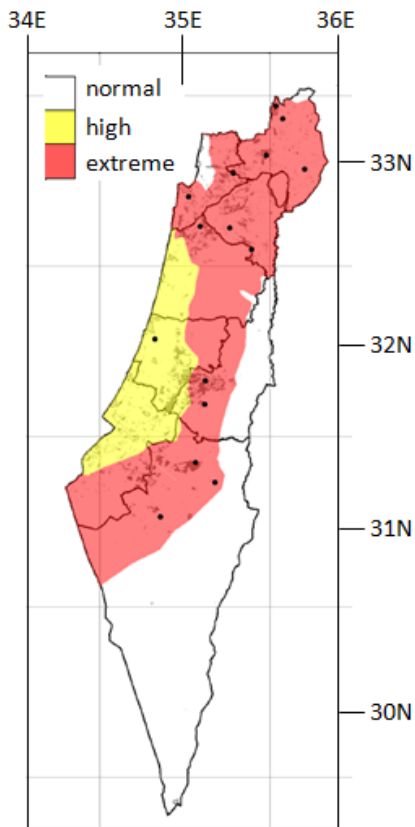


Fig. 1: The forecasted fire probability over Israel on May 30, 2013 (an extremely hot and dry day). Red indicates extreme risk with weather condition probability that occur less than 2% during the summer time. Yellow indicates high risk with probability of less than 10%. White indicates low fire risk.

### 2.1.2 Physical adaptation

- a. ECMWF deterministic model output is ingested to INCA (Integrated Nowcasting through Comprehensive Analysis) high resolution (1 km) nowcasting system (Haiden et. al. 2011) together with 81 meteorological stations.
- b. The short-range forecasting non-hydrostatic model COSMO ([www.cosmo-model.org](http://www.cosmo-model.org)) is running operationally with two domains. The first is of 7 km which is driven by the ECMWF global model IFS and second is 2.8 km resolution. Both model are run with assimilation cycles to ingest standard observations by nagging.

### 2.1.3 Derived fields

The global radiation from ECMWF forecasts is used to calculate the UV index by an empirical functions that connects between the global radiation and UV index. The forecast are displayed in an hourly forecast map (Fig. 2) in our web site.



# UV index forecast for the dates:

## 25/09/2015-26/09/2015

Calculation based on global radiation from ECMWF model

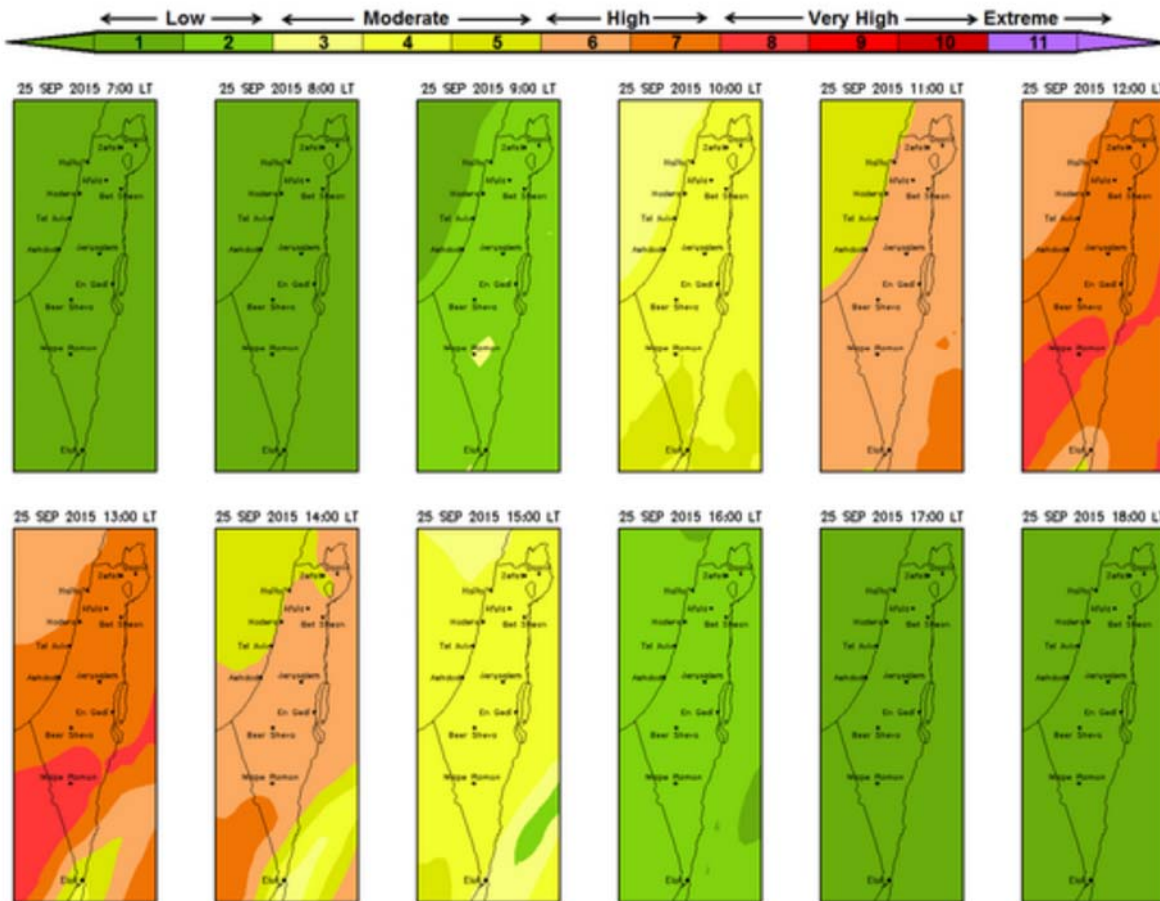


Fig 2: Hourly UV index forecasted for Israel.

### 2.2 Use of products

The main use of ECMWF products is as guidance in the medium term. The various output fields are made available to the forecaster. The Ensemble Prediction System (EPS) threshold probabilities, meteograms and Extreme Forecast Index (EFI) are used increasingly by the operational meteorologists to assess the likelihood of alternative forecast developments.

We use ECMWF fields as frame boundary conditions for COSMO forecasts (with the fields inserted every three hours).

### 3. Verification of products

#### 3.1 Objective verification

##### 3.1.1 Direct ECMWF model output (both deterministic and EPS)

###### Introduction

Israel has a Mediterranean climate with long, warm, rainless summers and relatively short, mild, rainy winters. The characteristics of the Israeli Climate are caused by Israel's location between the subtropical arid areas of the Sahara and the Arabian deserts, and the subtropical humid areas of the Levant and Eastern Mediterranean. The climate conditions are highly diverse within the state and depend locally on altitude, latitude, and the proximity to the Mediterranean Sea.

The ECMWF verification analysis was performed for the period Jan 1, 2014 – Dec 31, 2014 for two metrological stations: Bet Dagan (near Tel Aviv) and Jerusalem. These two stations represent the Israeli Mediterranean climate region. Bet Dagan climate is highly affected by the Mediterranean Sea, whereas Jerusalem climate is affected by both the sea and the topography of the central highlands. The next table summarizes the characteristics of these two stations:

	Longitude	Latitude	Height (m)	Height of the nearest grid point (m)	Distance from the coast (km)	Distance from nearest grid point (km)
Bet Dagan	34.814E	32.007N	35	64	7.6	5.81
Jerusalem	35.197E	31.770N	765	544	50.6	5.49

The verification analysis was performed for the meteorological parameters: temperature (at 2 meters), wind (at 10 meters) and precipitation (accumulated over 6 hours). Figures 3, 4, 5 present the Mean Bias Error (MBE, calculated as Forecast - Observed) and the Root Mean Square Error (RMSE) as function of the forecast range of the ECMWF (12 GMT + 0 hours till 12 GMT + 240 hours, with time steps of 6 hours). MBE and RMSE are presented by dashed and solid lines, respectively.

### a. Temperature forecast verification

Temperature forecast verification is presented on Fig. 3.

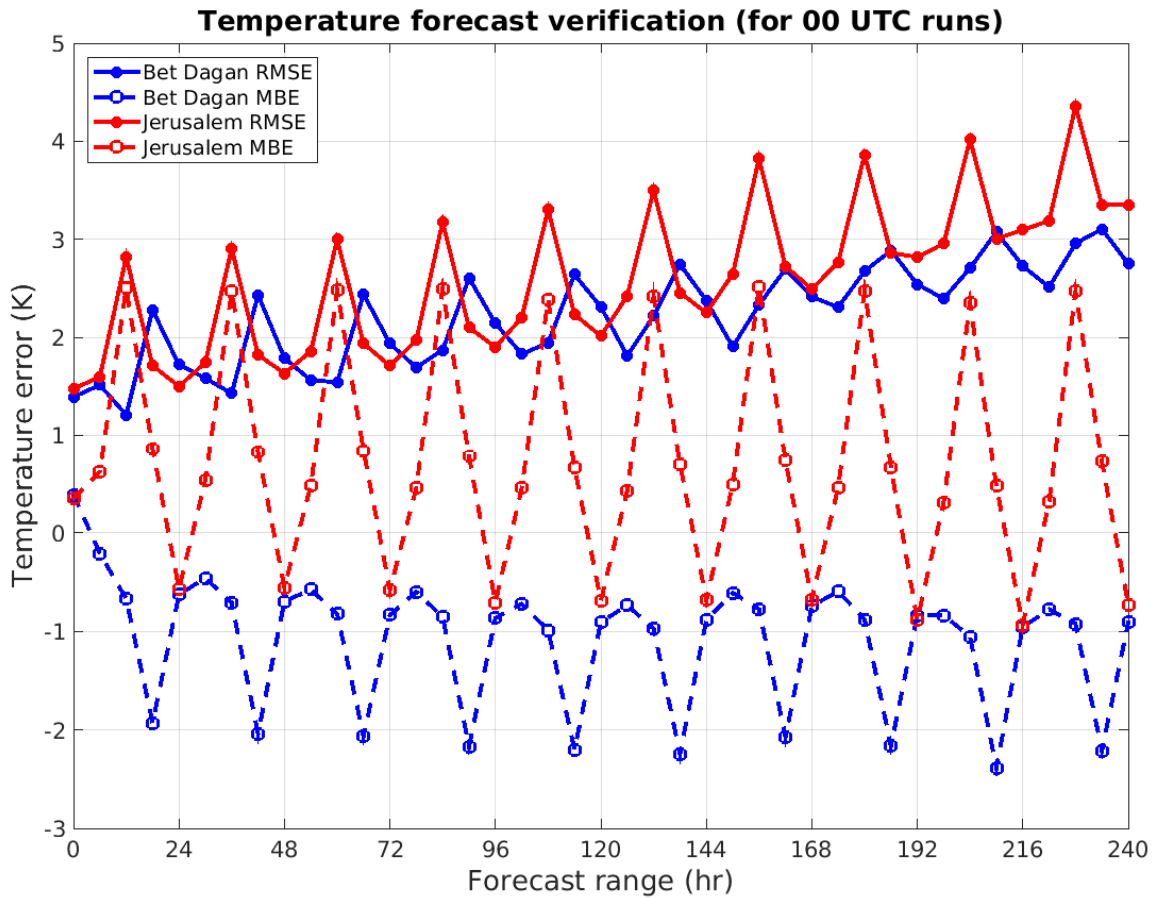


Fig. 3: Temperature forecast verification of ECMWF for Bet Dagan (near Tel Aviv) and Jerusalem for period 1.1.2014 –31.12.2014, based on 00Z runs.

For Bet Dagan at 12Z, 00Z and 6Z there is a negative bias of less than 1°C. For 18Z the bias is about 2°C, perhaps due to the rapid change during the sunset. During the day in Jerusalem there is a relatively high overestimation of the modelled temperature due to the lower grid point altitude. As expected, the RMSE increases with the forecast range, from about 2°C to 3-4°C. It might be of an interest to mention that in both scores (MBE and RMSE) there are oscillations as a function of the forecast hour. In Jerusalem the oscillations are more significant, and one can obviously see that at noon (12Z) the errors are larger than at night (0Z).

### b. Wind forecast verification

Wind forecast verification is presented in Fig. 4. For each forecast range the wind speed error  $|\overline{W}|_{forecast} - |\overline{W}|_{obs}$  was calculated during the entire period. MBE and RMSE were obtained for each of the two stations (Bet Dagan and Jerusalem).

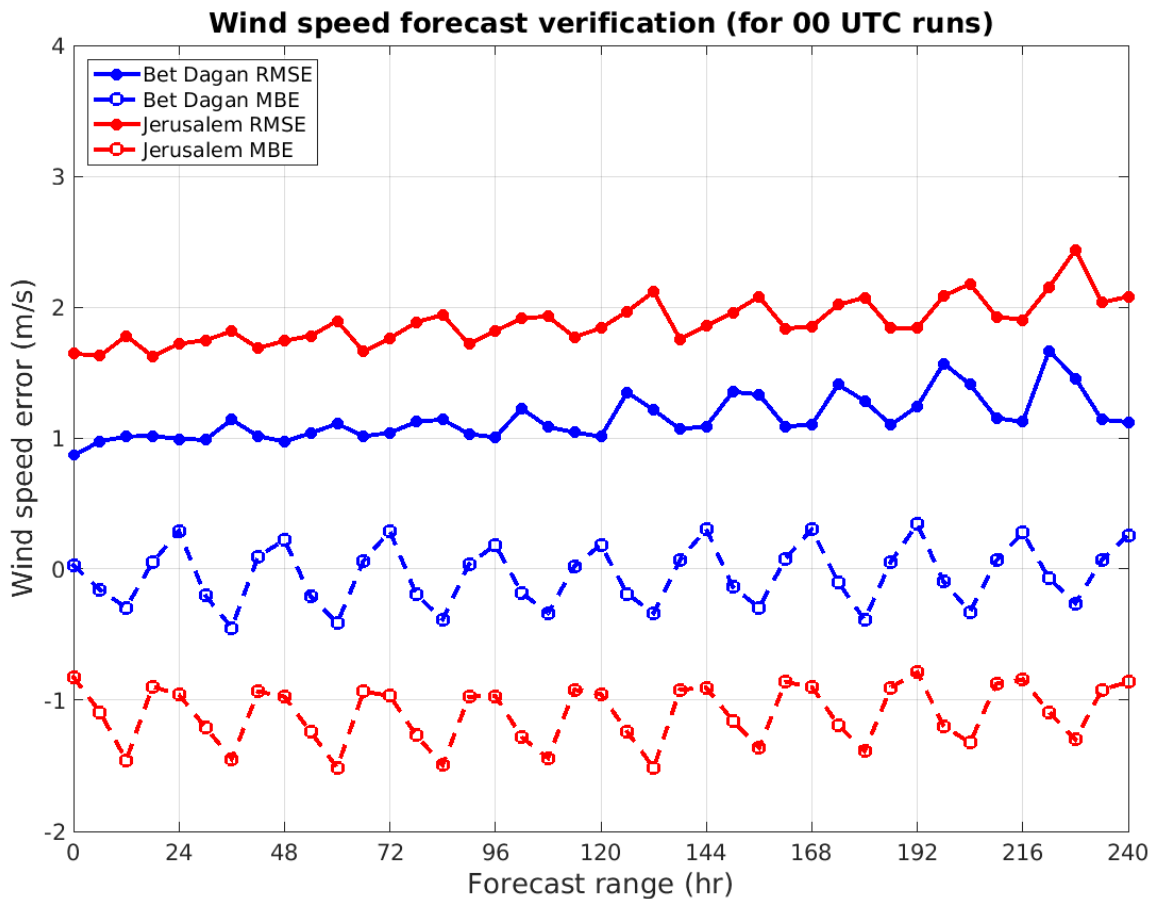


Fig. 4: Wind speed forecast verification of ECMWF for Bet Dagan (near Tel Aviv) and Jerusalem for period 1.1.2014 –31.12.2014, based on 00Z runs.

There is a negative bias in the wind speed for Bet Dagan 0-0.5 m/s and for Jerusalem 0.5-1 m/s. The RMSE increases with the forecast range: in Bet Dagan from ~1 m/s to ~2 m/s after 10 days; in Jerusalem from ~1.5 m/s to 2.8 m/s after 10 days. It could be explained by the coarse representation of the height of Jerusalem. Interesting to mention, that as in Fig. 3, in both scores (MBE and RMSE) there are diurnal oscillations. During the day (12Z) there is a systematic bias as the modelled wind is about 0.5-1 m/s weaker than the observed one. During the night (00Z) the bias is smaller, and the RMSE is smaller as well.

**c. Humidity verification**

Humidity forecast verification is presented in Fig. 5. At Bet Dagan at 00Z, 06Z and 12Z the bias is very small. At 18Z the bias is larger reaching a value of ~10%. This bias may be related to the temperature negative bias at 18Z (fig. 3). The RMSE increases form ~10% in the first day to ~20% after 10 days. For Jerusalem at night 00Z there is a small positive bias (+5%) while during the day at 12Z there is a small negative bias of 5%. The RMSE in Jerusalem seems to deteriorate with time stronger compared to Bet Dagan.

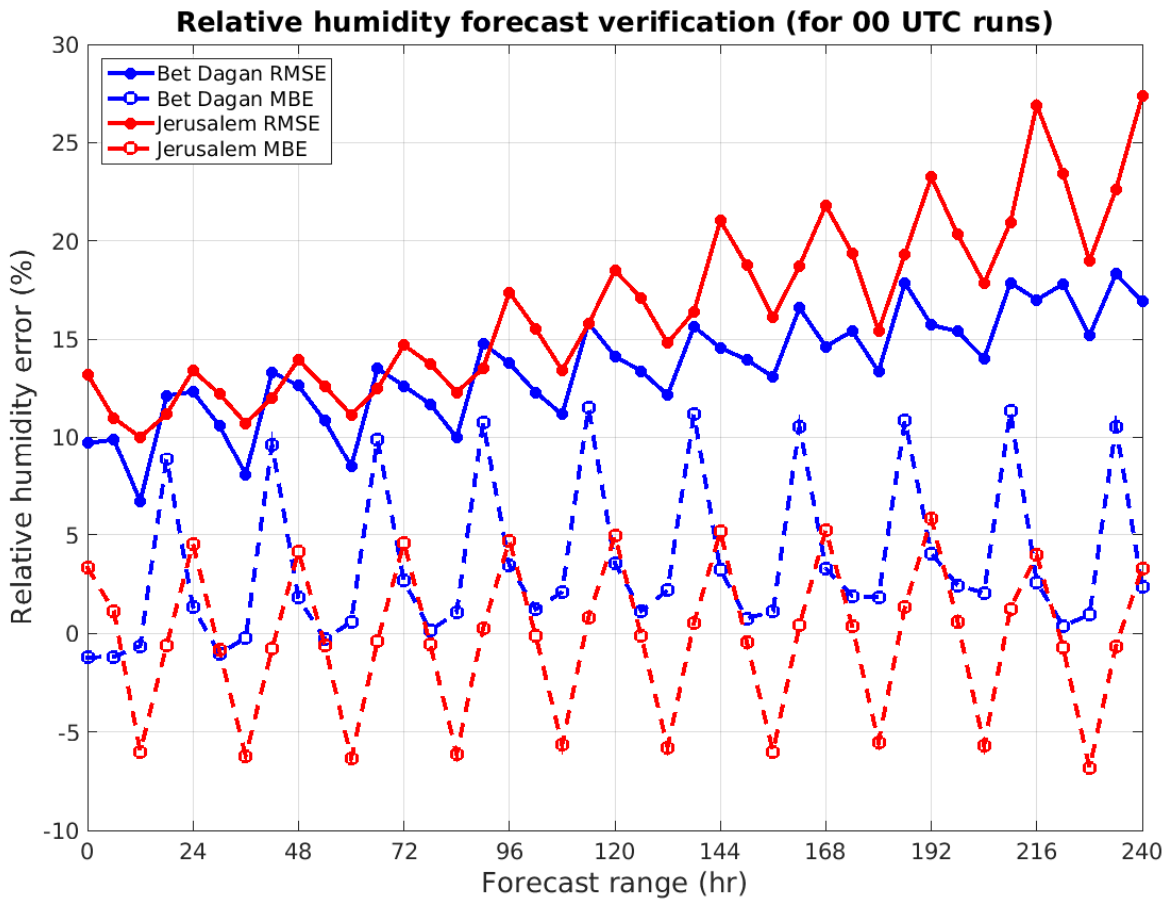


Fig. 5: Relative humidity forecast verification of ECMWF for Bet Dagan (near Tel Aviv) and Jerusalem for period 1.1.2014 –31.12.2014, based on 00Z runs.

#### d. Wave model

The ECMWF WAM high-resolution Limited Area Wave (LAW) forecast model (hereafter EC WAM) has been evaluated by analyzing Significant Wave Height (SWH) data. SWH from two buoys were compared with the model SWH values taken from a “native” grid point near each buoy. The buoys are located in Haifa (32.844°N, 34.938°E) and in Ashdod (31.875°N, 34.649°E). The nearby native grid points selected for the comparisons are at (32.900°N, 34.955°E) and (31.900°N, 34.573°E) for Haifa and Ashdod, respectively.

Fig. 6 shows very high correlations ( $CC=0.94-0.95$ ) between the ECMWF WAM forecast and the buoy observations, based on 2014 data. An overall 6% underestimation is found at each location. The WAM underestimation is more pronounced at high SWH. Analyzing data from three years combined yield similar results. Based on 2012-2014 data, the model underestimates the heights relative to the buoy by 6% and 4% for Haifa and Ashdod, respectively. For both locations a  $CC=0.96$  is obtained.

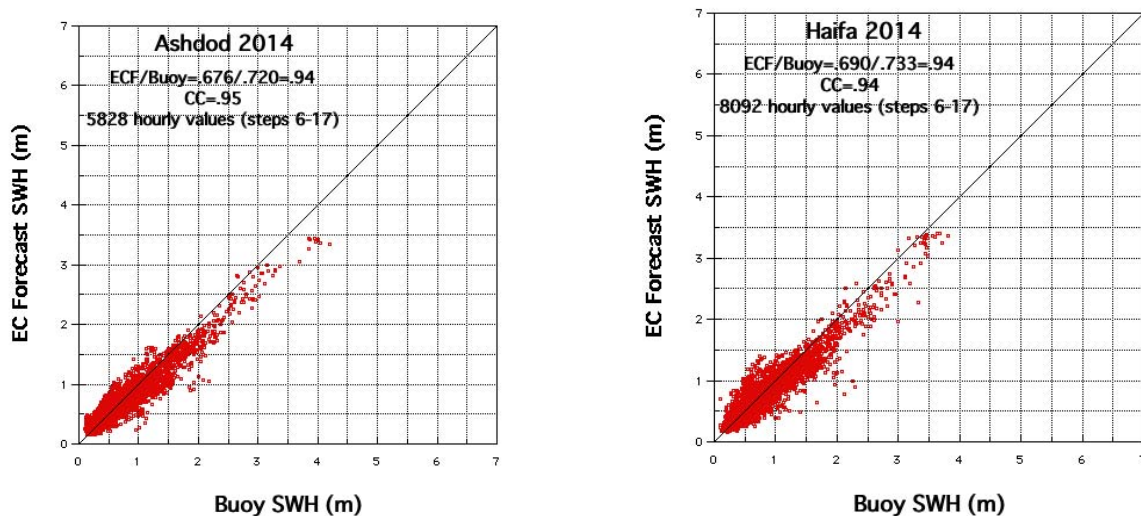


Fig. 6. The 2014 EC WAM Significant Wave Heights near Ashdod (left) and Haifa (right) buoys vs. the buoy hourly-interpolated heights. Model data are based on base+6-hr till base+17-hr, and therefore, represent the most continuous short term forecast available.

**d. System 4 Seasonal forecast verification**

Table 2 presents the seasonal forecast probabilities for Above-normal, Normal and Below-normal conditions for central and northern Israel. As JJA is dry, the precipitation forecast is not relevant. The Rank Probability Skill Score (RPSS) compared to an equal probability forecast (climatology) indicates that only for the DJF temperature the forecast was skilful. For DJF precipitation and JJA temperature the forecast skill was negative. The RPSS values vary from 1 for a perfect forecast (100% probability for the observed tercile) to -3.5 for a busted forecast.

Table 2: A summary of the ECMWF system 4 forecast for central and northern Israel, observed and Ranked Probability Score skill (RPSS).

	JJA 2014			DJF 2014-2015			Observed	RPSS		
	Forecast			Forecast						
<b>Precipitation</b>	----			0			----			
				A	N	B	above	0.16		
			37	37	26	normal				
<b>Temperature</b>	A	N	B	above			0.75			
	63	31	6	normal			A	N	B	above
			47	33	20	normal				

3.1.2 ECMWF model output compared to other NWP models

Here we present the temperature (at 2m) verification of 5 models run/received at IMS:

- IFS 0.125NX0.125E degrees resolution,
- GME 0.25NX0.25E degrees resolution (as obtained in IMS).
- UKMO 0.833NX0.555E degrees resolution (as received in IMS),
- COSMO-ME (Italy) 0.0625NX0.0625E resolution (boundary and initial conditions – ECMWF)
- COSMO-IL 0.025NX0.025E degrees resolution (boundary and initial conditions - ECMWF),

Figs. 7 and 8 present the 2014 Root Mean Square Error (RMSE) as function of the diurnal time, for Bet Dagan and Jerusalem stations, respectively.

The higher resolution of the COSMO model is reflected in a lower average RMSE compared to the IFS especially is the mountainous station of Jerusalem. The COSMO-ME model which includes data dissimilation has a better average RMSE score compared to the COSMO\_IL that at this period was still running without data assimilation.

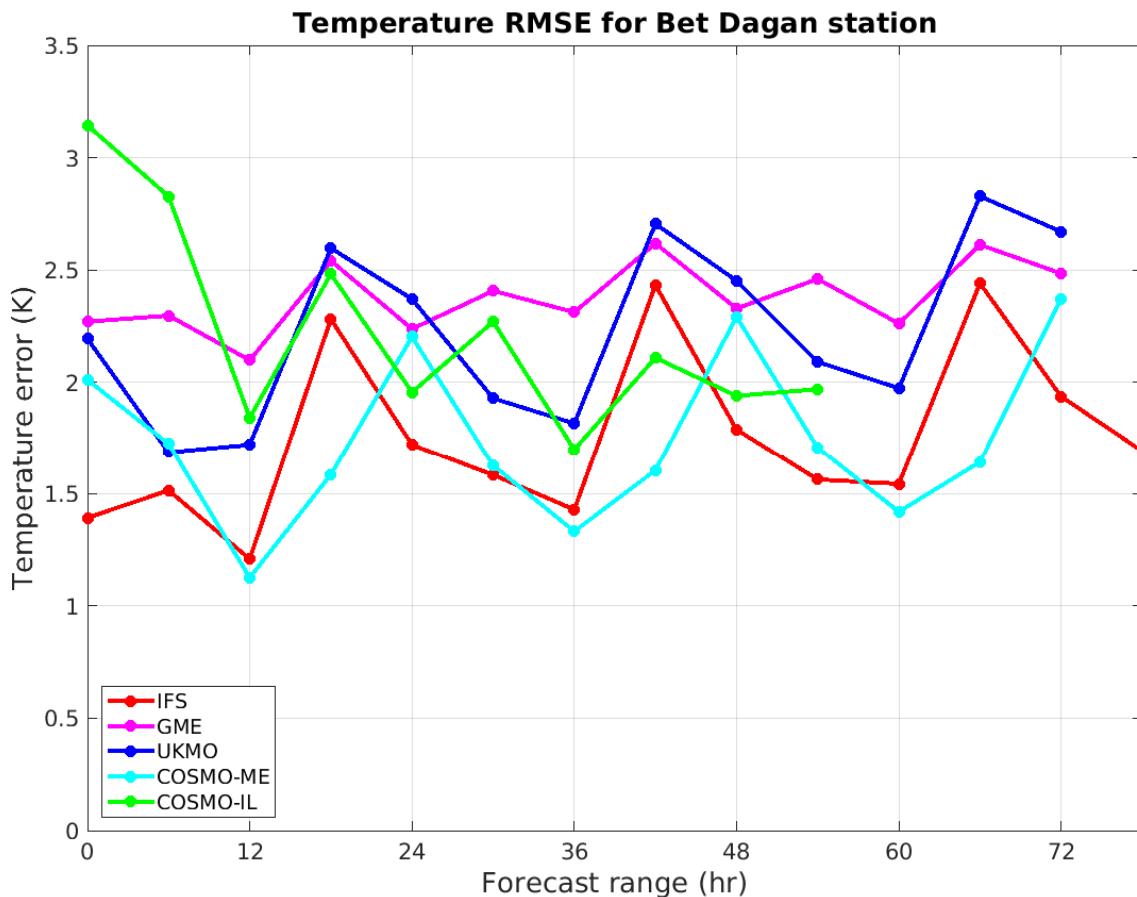


Fig. 7: The RMSE for temperature forecasts by 6 models received for at Bet Dagan (near Tel Aviv) for the period 1.1.2014 – 31.12.2014, based on the 00 UTC runs.

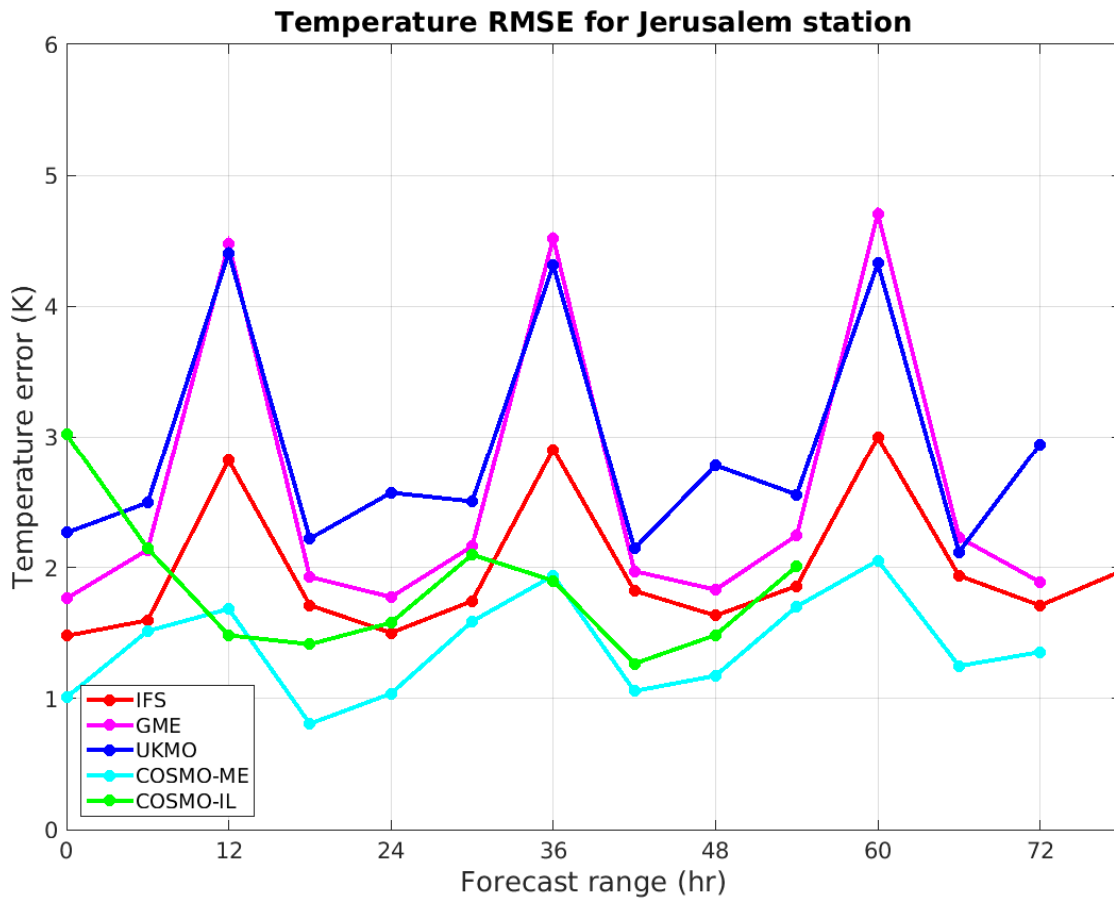


Fig. 8: As Fig. 7 for Jerusalem.

### 3.1.4 End products delivered to users

## 3.2 Subjective verification

### 3.2.1 Subjective scores (including evaluation of confidence indices when available)

### 3.2.2 Synoptic studies

## 4. References to relevant publications

Haiden, T., A. Kann, C. Wittmann, G. Pistotnik, B. Bica, C. Gruber, 2011: The Integrated Nowcasting through Comprehensive Analysis (INCA) System and Its Validation over the Eastern Alpine Region. *Wea. Forecasting*, **26**, 166–183.